

Experimental and mechanistic study on the enhanced CO₂ capture using adjustable choline chloride-based DES

By Jiaqiang Wang^{1,2}, Dexin Liu^{1,2*},

ABSTRACT:

Excessive emissions of carbon dioxide (CO₂) in the environment have become a major factor contributing to global warming. The development of efficient, green, and sustainable absorbents for CO₂ capture is urgently needed. In this study, a series of deep eutectic solvents (DES) were prepared by using choline chloride (ChCl) as the hydrogen bond acceptor (HBA) and ethylene glycol (Eg), glycolic acid (Gla), and monoethanolamine (MEA) as hydrogen bond donors (HBDs), each containing different HBDs. The results showed that the CO₂ capture performance of the DESs containing different HBDs exhibited significant variations. Among them, the amino-type HBD (MEA) demonstrated the best absorption capacity at room temperature (1.65 mol CO₂/kg DES), while non-amino-type HBDs (Eg, Gla) consistently followed the trend: Gla > Eg. In addition, this work combined FTIR, NMR, DFT calculations, and molecular dynamics simulations to reveal, from a microscopic perspective, the intrinsic mechanisms behind the differential CO₂ capture abilities of the adjustable HBDs. Overall, this work reveals the significant contribution of the tunable HBDs to CO₂ capture in DESs from a microscopic mechanistic perspective, providing a direction for the future development of green DESs with high absorption capacity.

Keywords: CO₂ capture, DES, HBD, DFT calculations, Molecular dynamics

1. Introduction

The exacerbation of environmental climate issues and global warming has become one of the major problems that urgently need to be addressed. The primary cause of this issue is the large-scale emission of greenhouse gases, particularly carbon dioxide (CO₂), into the atmosphere. By 2021, the average concentration of CO₂ in the atmosphere had exceeded 415 ppm (Xin et al., 2025). Among the numerous sources of CO₂ emissions, coal-fired power plants, as fixed emission sources, release a significant amount of CO₂ annually. To achieve carbon capture and storage (CCS) goals. Among them, CO₂ absorption and reutilization are considered the most promising technologies for achieving carbon neutrality. However, traditional amine aqueous solutions, while exhibiting high absorption capacities, inevitably suffer from degradation and corrosion of equipment during high-temperature applications, leading to a significant reduction in absorption performance and a sharp increase in maintenance costs (Valencia-Marquez et al., 2017). In the relevant reports, the Deep Eutectic Solvent (DES) solution still maintains a loading capacity of approximately 80% after ten cycles of regeneration. In contrast, the traditional

¹ School of Petroleum Engineering, China University of Petroleum (East China), China;

² School of Petroleum Engineering, China University of Petroleum (East China), China.

*Corresponding author.

aqueous monoethanolamine (MEA) solution only retains a loading capacity of 47.65% after ten regenerations (Mao *et al.*, 2025). It is fully demonstrated that the hydrogen bonds between DES inhibit volatilization and reduce the vapor pressure, thereby ensuring excellent reusability. To overcome the limitations of using amine solutions, it is crucial to develop low-cost, recyclable, and efficient green absorbents.

Ionic liquids (ILs) have emerged as a new type of green CO₂ capture solvent (Palomar *et al.*, 2024). However, the high cost of ionic liquids, the complex and time-consuming synthesis processes are limiting factors. DESs, which possess similar physicochemical properties to ILs, offering simpler synthesis, lower costs, and tunable structures—thus providing new possibilities.

The characteristics of both HBA and HBD are crucial in determining the CO₂ capture capacity of DESs (Zhou *et al.*, 2024). DESs based on ethylene glycol (Eg) and glycolic acid (Gla) exhibit relatively weak hydrogen bond networks, resulting in lower viscosity and relatively poor absorption capacity. However, they demonstrate excellent desorption performance. Therefore, Eg and Gla were selected as the other two HBDs. ChCl is a common HBA in DESs and has been extensively studied due to its low cost, non-toxicity, and environmentally friendly properties.

DFT calculations and molecular dynamics (MD) simulations provide a more detailed understanding of the CO₂ absorption mechanisms in DESs. Jafari *et al.* (Jafari *et al.*, 2025) used MD simulations to study the ChCl/para-toluenesulfonic acid (PTSA)-DES system at different molar ratios, investigating the effects of water content and temperature on the viscosity of DESs and the interaction energy with CO₂. Molecular dynamics simulations can break through the constraints of real-world conditions, exploring related mechanisms at the molecular level.

This study systematically reports the preparation of a series of DESs with different hydrogen bond donors (HBDs) such as Eg, Gla, and MEA, and ChCl as the HBA. Exploring the interaction mechanism between Deep Eutectic Solvents (DESs) and carbon dioxide (CO₂) using DFT calculations and MD simulations. In addition, a study was conducted to investigate the interactions between water, DES components and carbon dioxide, and the effect of water content on the interaction energy between DES components and carbon dioxide was analyzed. This study reveals the intrinsic mechanism of the different carbon dioxide capture capacities of tunable hydrogen bond extractants from both theoretical and experimental aspects, paving the way for the design of tunable HBD extractants with different HBDs for CO₂ removal.

2. Materials and Methods

2.1 Materials

Choline chloride (ChCl, 98%), glycolic acid (Gla, 99%), and ethylene glycol (Eg, 99%) were purchased from Aladdin Reagent Co., Ltd. (Shanghai, China). PEG-200 and magnesium sulfate (MgSO₄, 99%) were obtained from Sinopharm Group Co., Ltd. (Shanghai, China). All reagents were of analytical grade and were used without further purification.

2.2 Preparation of DESs

The HBA and HBD were mixed in a certain molar ratio (HBA: HBD = 1:2) and ultrasonicated for 15 minutes. The mixture was then placed in an 80°C oil bath and reacted under a nitrogen atmosphere for 4 hours until a homogeneous and stable transparent liquid was formed. The product was subsequently dried under vacuum at 60°C for 20 hours to remove excess water and volatile substances, yielding the final product actions.

2.3 CO₂ Absorption and Desorption

The absorption experiments were conducted at 273.15 K, 303.15 K, and 328.15 K, with a total mass of 10 g for the absorption system and H₂O: DES ratios of 8: 2, 7.5: 2.5, and 7: 3. The gas flow rate was 40-50 mL·min⁻¹. Absorption columns containing varying amounts of DES were partially immersed in a thermostatic water bath set to the desired temperature. Simulated flue gas was bubbled into the DES. Desorption experiments were carried out at 353.15 K, with a nitrogen flow rate of 40-50 mL·min⁻¹. CO₂ absorption and desorption capacities were periodically monitored gravimetrically using an electronic balance with a precision of 0.1 mg. The absorption apparatus is shown in Figure 1.

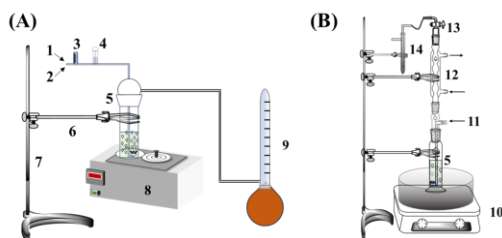


Figure 1: Experimental setup for CO₂ absorption (A) and desorption (B): (1-2) high-purity CO₂; (3) rotameter; (4) magnesium sulfate bottle (for removing residual moisture); (5) bubble absorption column; (6) tube clamp; (7) iron stand; (8) water bath; (9) soap film flowmeter; (10) oil bath; (11) N₂; (12) condenser; (13) adapter; (14) oil bubble tube.

2.4 Theoretical Calculations

2.4.1 DFT Calculations

Quantum chemical calculations were performed using the Gaussian 16 program to elucidate the interactions between DESs and between DESs and CO₂. The structures were optimized at the M06-2X (D3)/6-311G(d,p) level of theory without imaginary frequencies, and single-point energies were calculated for the interactions between DES and CO₂ at the M06-2X (D3)/6-311++G(d,p) level (Du et al., 2025; Frisch et al., 2016). The solvent effect was simulated using the Solvation Model based on Density (SMD). The wavefunction files were analyzed using the Multiwfn 3.8 program (Lu & Chen, 2012).

2.4.2 Molecular Dynamics (MD) Simulations

MD simulations were performed using GROMACS 2023.4 software to simulate and analyze the CO₂ absorption process by the prepared DESs at ambient temperature and pressure. The AMBER force field was used to handle bonded and non-bonded interactions, the SPC/E model was applied to describe water molecules, and the TraPPE model was used to represent CO₂ molecules (Zhao et al., 2025).

This study was conducted in three stages: energy minimization, pre-equilibration, and production simulation. The initial box structure is shown in Table 1. Energy minimization was performed using the steepest descent method with a step size of 0.002 ps, for a maximum of 10,000 steps, to obtain a reasonable initial structure. The system was then heated to the target temperature and maintained constant using the NPT ensemble for the first 50 ps. Subsequently, a 1000 ps MD simulation was performed for the equilibration stage. The system was run for 10 ns under Parrinello-Rahman pressure coupling and a velocity rescaling thermostat to reach the production phase.

Table 1: Details of molecular dynamics simulation systems.

System	CO ₂ loading (mol/kg)	Simulation box	Box length (Å)
30 wt% ChCl-2Eg-CO ₂	0.30	1000H ₂ O:40ChCl:80Eg:40CO ₂	38.1324
30 wt% ChCl-2Gla-CO ₂	0.40	1000H ₂ O:40ChCl:80Gla:40CO ₂	38.1128
(30 wt% ChCl-2MEA)	1.65	1000H ₂ O:40ChCl:40MEACOO ⁻ :40 MEAH ⁺	38.5037

3. Results and Discussion

3.1 Effect of Water Content on the CO₂ Absorption Capacity of DESs

To investigate the effect of water content on the absorption performance, DES solutions with different water contents were prepared. Specifically, DES mixtures with mass concentrations of 20 wt%, 25 wt%, and 30 wt% were selected (20 wt% DES refers to a mixture of 2.0 g DES and 8.0 g H₂O). The results showed that CO₂ absorption capacity increased with the increase in DES content. Compared to the 20 wt% (Figure 2(A)) and 25 wt% (Figure 2(B)) DES absorption solutions, Figure 2(C) shows that the CO₂ loading capacity of 30 wt% ChCl-2Eg, ChCl-2Gla, and ChCl-2MEA reached maximum values of 0.301, 0.398, and 1.65 mol CO₂/kg DES, respectively. This indicates that the adjustment of the HBD leads to significant differences in CO₂ absorption, always following the order of MEA > Gla > Eg at different mass concentrations. The effect of water content is primarily reflected in environments with higher water content, where water, as a solvent molecule, is confined within the pores of the DES and interacts with the DES molecules through hydrogen bonding. This not only enhances the mobility and absorption kinetics of the DES molecules but also maintains the structural integrity of the DES (Lukasheva *et al.*, 2024). Choline chloride-based DESs containing tertiary amines cannot directly interact with CO₂ under anhydrous conditions. However, under humid conditions, the mass transfer between CO₂ and DES is more readily driven, facilitating the formation of carbamate bonds between the amine groups and CO₂. This does not imply that lower water content is preferable. Lower water content leads to higher costs; the reduction of water content causes a sharp increase in viscosity after DES molecules absorb a portion of CO₂, which makes molecular diffusion more difficult and significantly affects

subsequent CO₂ absorption performance. Based on these results, 30 wt% DES both maintains a humid environment and ensures a higher DES content in the solution, allowing the tertiary amine groups to effectively promote the reaction between MEA and CO₂. The viscosity after CO₂ absorption did not significantly increase, facilitating molecular diffusion. Unless stated otherwise, 30 wt% DES was selected for subsequent experiments.

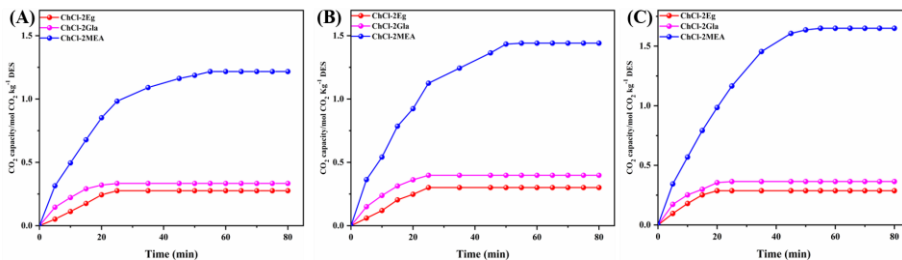


Figure 2: CO₂ absorption performance of 20 wt% (A), 25 wt% (B), and 30 wt% (C) DES at ambient temperature and pressure.

3.2 Effect of Temperature on CO₂ Absorption Capacity

Temperature plays a significant role in the CO₂ absorption process. As shown in Figures 3(A)-(C), this figure explores the trend of CO₂ absorption capacity at different temperatures for different HBDs. The results show that the CO₂ absorption capacity of 30 wt% DESs decreases with increasing temperature, but the absorption capacity still follows the order: MEA > Gla > Eg, with MEA exhibiting more pronounced fluctuations due to temperature effects. The viscosity and absorption capacity of the corresponding DESs before and after CO₂ absorption are compared. Notably, due to the reduction in absorption energy, the absorption of CO₂ by the prepared DES is an exothermic process. However, increasing the temperature leads to a decrease in viscosity and an increase in the flowability of the DES, thereby enhancing the exposure of absorption sites. When the absorption reaches saturation, it cannot compensate for the CO₂ lost during desorption. Therefore, CO₂ absorption at high temperatures is irreversible.

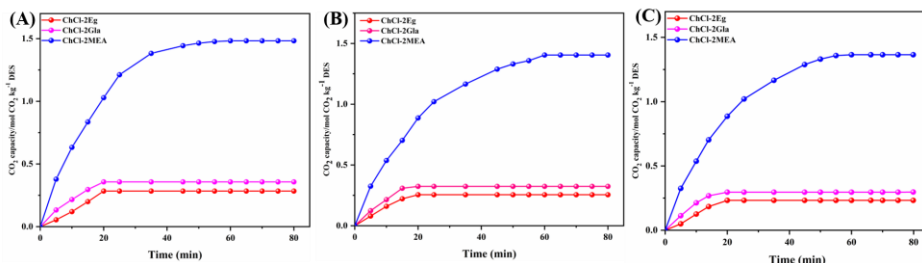


Figure 3: CO₂ absorption performance of DES at (A) 303.15 K, (B) 308.15 K, and (C) 313.15 K.

3.4 Absorption Mechanism

3.4.1 NMR and FTIR

To validate the successful preparation of different DESs and explore the CO₂ absorption mechanism, Figure 5 shows the ¹H NMR and ¹³C NMR spectra of DESs with different HBDs before and after CO₂ capture. As shown in Figures 5(A)-(C), the

differences in the ^1H NMR spectra of the three types of DESs before and after CO_2 capture are not significant. The main changes observed are chemical shifts, with peak intensity and peak area remaining almost unchanged, which can primarily be attributed to changes in hydrogen bonding. For example, in ChCl-2Gla, the chemical shift of the hydroxyl group in the carboxyl group shifted from 8.35 ppm to 8.43 ppm before CO_2 absorption (Figure 5(B)), but the peak area and intensity remained unchanged. In the ^{13}C NMR of ChCl-2MEA after CO_2 absorption, a distinct new peak was observed (Figure 5(F)), and its intensity and peak area differed from others. A new signal at 164.73 ppm appeared, which was mainly due to the formation of N-COO^- , indicating that amine-based HBDs (MEA) facilitate chemical absorption of CO_2 (Han *et al.*, 2024). Furthermore, the chemical shifts of C-1, C-2, and C-3 moved from 53.86 ppm to 54.10 ppm, and C-4 shifted from 67.40 ppm to 67.54 ppm after CO_2 absorption, which indicates a chemical shift due to CO_2 absorption on the DES surface. Comparing different HBDs, the new peak observed in amine-based HBD (MEA) is the most significant, further demonstrating that the DES formed by ChCl-2MEA exhibits the best CO_2 absorption capacity. Therefore, the results above indicate that the modulation of HBDs has a positive impact on CO_2 absorption and is, to some extent, constrained by the regulation of HBDs.

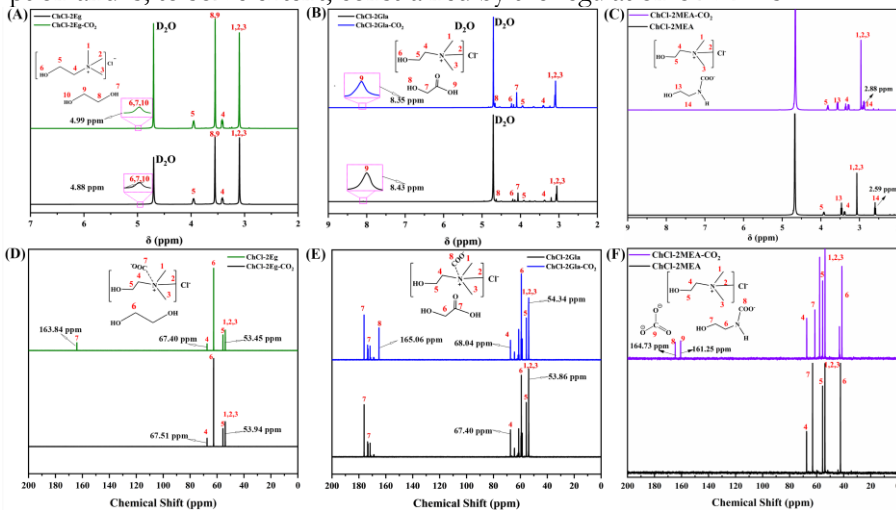


Figure 5: ^1H NMR/ ^{13}C NMR spectra before and after CO_2 absorption: ChCl-2Eg/ChCl-2Eg- CO_2 (A)/(D), ChCl-2Gla/ChCl-2Gla- CO_2 (B)/(E), ChCl-2MEA/ChCl-2MEA- CO_2 (C)/(F).

FTIR spectra before and after CO_2 absorption were compared to further investigate the interaction between DES and CO_2 . As shown in Figure 6, significant differences in the characteristic peaks of each DES were observed before and after CO_2 absorption. For the non-amino HBD, ChCl-2Eg, a characteristic peak at 3202.56 cm^{-1} , attributed to the $-\text{OH}$ stretching vibration, shifted to 3403.77 cm^{-1} after CO_2 absorption, indicating that CO_2 absorption is likely influenced by hydrogen bonding. In contrast, ChCl-2MEA exhibited new characteristic peaks at 1563.92 cm^{-1} and 1331.14 cm^{-1} after CO_2 absorption, primarily due to the asymmetric stretching vibration of $-\text{COO}^-$ and the stretching vibration of the $-\text{NCOO}^-$ group (C. Wang *et al.*, 2024). Additionally, the signal peak at 1483.92 cm^{-1} in ChCl-2MEA was enhanced, attributed to the increased $-\text{CH}_2-$ bending vibration after the formation of $-\text{NCOO}^-$ on the $-\text{NH}_2-$ group near the methylene.

This result indicates that ChCl-2MEA forms multiple new absorption products with CO₂, and the absorption is controlled by more significant chemical interactions.

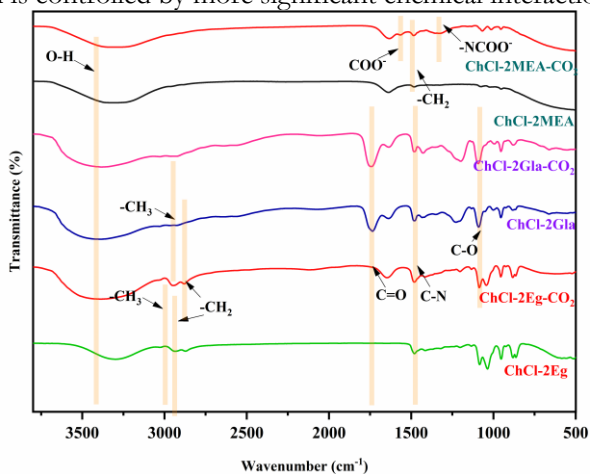


Figure 6: FTIR spectra of DES before and after CO₂ absorption.

3.4.2 DFT Calculation

This study comprehensively analyzed the influence of hydrogen bond acceptors (HBAs) in DES on CO₂ absorption performance using density functional theory (DFT). Initially, the interactions between ChCl and three different hydrogen bond donors (HBDs) were examined by adjusting the types of HBDs. Subsequently, various microscopic analysis methods were used to explore the interactions between different DESs and CO₂, revealing how variations in HBD influence CO₂ absorption. This provides a detailed theoretical foundation for the future development of functional green absorbents. Figures 7(A)-(B), Figures 8(A)-(B), and Figures 9(A)-(B) display the optimized geometric structures of the DES and DES-CO₂ complexes based on selected HBAs and HBDs. As shown in Figures 7(C)-(E), Figures 8(C)-(E), and Figures 9(C)-(E), the red areas in the ESP map represent regions with a high concentration of negative charge, while the blue areas indicate regions with a higher density of positive charge. Notably, the oxygen atoms on the three HBDs are located in the red regions, suggesting that electron density redistribution may occur in these areas, which effectively promotes CO₂ absorption. The vdW potential analysis between DES and CO₂ is also of considerable practical significance due to the weak molecular polarity between CO₂ and DES. The vdW potential minima for ChCl-2MEA, ChCl-2Eg, and ChCl-2Gla are -1.50, -1.42, and -1.58 kcal/mol, respectively, and are distributed above and below the DES, indicating favorable CO₂ absorption as shown in Figures 7(E), Figures 8(E), and Figures 9(E). Compared to ChCl-2MEA-CO₂ and ChCl-2Eg-CO₂, ChCl-2Gla-CO₂ exhibits the lowest vdW potential minima, indicating the strongest vdW interaction between ChCl-2Gla-CO₂. In addition, frontier molecular orbital (FMO) theory was used to analyze the distribution of the lowest unoccupied molecular orbital (LUMO) and highest occupied molecular orbital (HOMO) of DES and DES-CO₂. The energy gap (E_{gap}) can indicate the stability of the DES-CO₂ complex. As shown in Figures 7(F), Figures 8(F), and Figures 9(F), compared to the E_{gap} of DES, the E_{gap} of the three DES-CO₂ complexes shows an increasing trend. After CO₂ absorption,

the charge distribution in the complex becomes more uniform, and the structure becomes more stable.

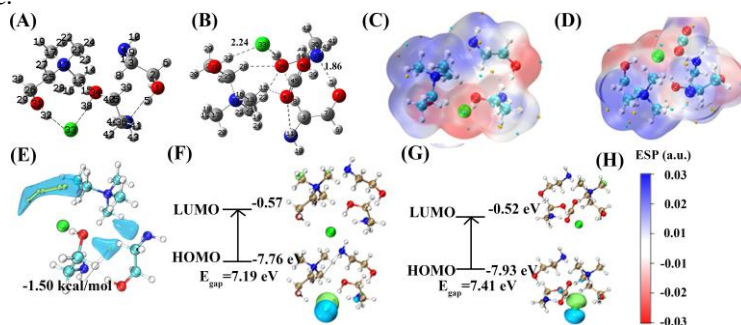


Figure 7: Optimized geometric structures of *CbCl-2MEA* (A) and *CbCl-2MEA-CO₂* (B). ESP of *CbCl-2MEA* (C) and *CbCl-2MEA-CO₂* (D). vdW potential of *CbCl-2MEA-CO₂* (E). LUMO and HOMO orbitals of *CbCl-2MEA* (F) and *CbCl-2MEA-CO₂* (G). Distribution of ESP (H).

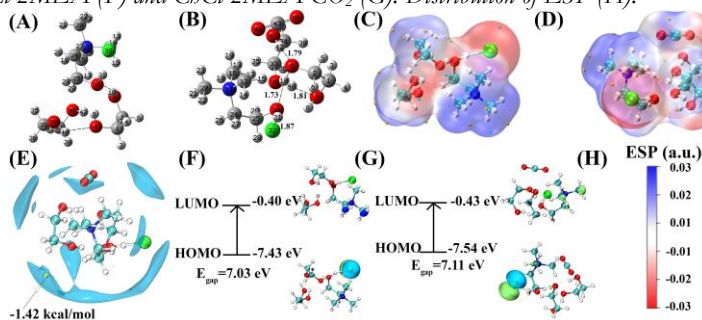


Figure 8: Optimized geometric structures of *CbCl-2Eg* (A) and *CbCl-2Eg-CO₂* (B). ESP of *CbCl-2Eg* (C) and *CbCl-2Eg-CO₂* (D). vdW potential of *CbCl-2Eg-CO₂* (E). LUMO and HOMO orbitals of *CbCl-2Eg* (F) and *CbCl-2Eg-CO₂* (G). Distribution of ESP (H).

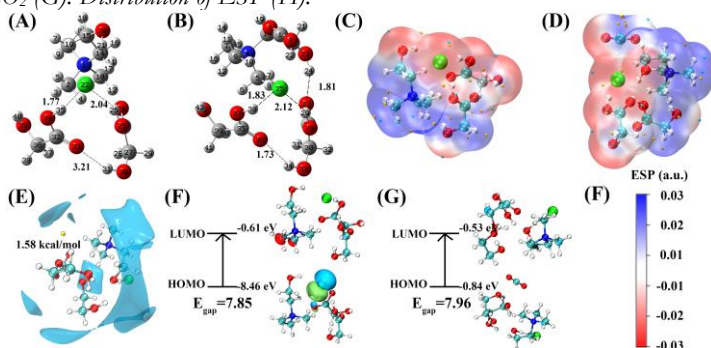


Figure 9: Optimized geometric structures of *CbCl-2Gla* (A) and *CbCl-2Gla-CO₂* (B). Electrostatic potential maps of *CbCl-2Gla* (C) and *CbCl-2Gla-CO₂* (D). vdW potential of *CbCl-2Gla-CO₂* (E). LUMO and HOMO orbitals of *CbCl-2Gla* (F) and *CbCl-2Gla-CO₂* (G). Distribution of ESP (H).

In AIM theory, bonds refer not only to chemical bonds within molecules but also to bonds formed by weak interactions between molecules. Figures 10(A), 10(E), and 10(I) display the topological structures of electron density for *ChCl-2MEA*, *ChCl-2Gla*, and *ChCl-2Eg* with CO_2 , illustrating that there are molecular bonds between the HBD and HBA, as well as between DES and CO_2 , indicating intermolecular interactions between

DES and CO₂. Additionally, to clearly demonstrate the van der Waals surface interaction strength between DES and CO₂, the electrostatic interaction characteristics between DES and CO₂ were analyzed. As shown in Figures 10(B), 10(F), and 10(J), it can be clearly observed that there is electrostatic potential complementarity between ChCl-2Gla, ChCl-2Eg and CO₂. The positive electrostatic potential in CO₂ interacts with the negative electrostatic potential in DES, with the van der Waals surface penetration distances for ChCl-2Eg, ChCl-2Gla, and ChCl-2MEA with CO₂ being 2.16 Å, 1.60 Å, and 1.88 Å, respectively.

Through the IGMH analysis, the interaction regions between the absorption liquid and CO₂ were qualitatively revealed. As shown in Figures 10(C), 10(G), and 10(K), the isosurfaces are alternately displayed in blue, green, and red, where blue represents the strongest hydrogen bonding, green indicates strong van der Waals interaction, and red represents repulsion. This provides a clear visual distinction of the interaction regions between different DESs and CO₂. Furthermore, the scatter plots for the interactions between DES and CO₂, shown in Figures 10(D), 10(H), and 10(L), quantitatively reveal the intensity of the weak interactions between the two. In all scatter plots, when $\text{sign}(\lambda_2)\rho$ is between -0.05 and -0.03 a.u., it is evident that there is strong hydrogen bonding (e.g., O-H···O, O-H···Cl) between HBA and HBD, with values reaching a maximum peak of 0.06-0.08 a.u. For the interactions between CO₂ and the three types of DESs, the van der Waals interaction is strongest between ChCl-2Gla and CO₂, reaching up to 0.05 a.u. Therefore, these results confirm that the modulation of HBDS significantly affects the weak interactions between CO₂ and DES, and these interactions play a significant role in determining the CO₂ absorption capacity on the DES surface.

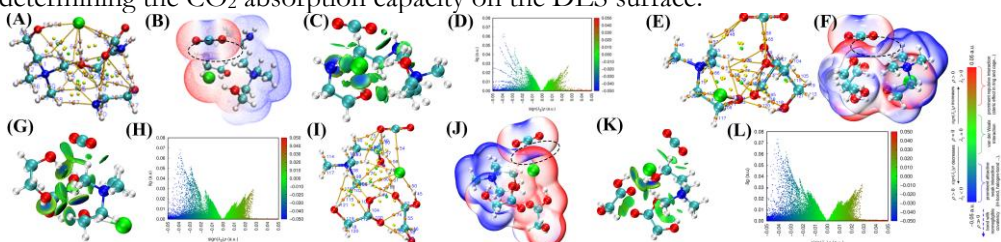


Figure 10: Electronic density topology structures of ChCl-2MEA-CO₂ (A), ChCl-2Eg-CO₂ (E), and ChCl-2Gla-CO₂ (I) (orange spheres: BCP; orange lines: intermolecular bond diameter). VdW surface penetration maps for ChCl-2MEA-CO₂ (B), ChCl-2Eg-CO₂ (F), and ChCl-2Gla-CO₂ (J). IGMH maps for ChCl-2MEA-CO₂ (C), ChCl-2Eg-CO₂ (G), and ChCl-2Gla-CO₂ (K). Scatter plots for ChCl-2MEA-CO₂ (D), ChCl-2Eg-CO₂ (H), and ChCl-2Gla-CO₂ (L).

3.4.3 MD Simulation

There are significant differences in hydrogen bonding before and after CO₂ absorption in DESs. To analyze the distribution of hydrogen bonds in different HBDS, the number and lifetime of hydrogen bonds within the system were examined. As shown in Figure 11, initially, the differences in the number of hydrogen bonds and hydrogen bond lifetimes in the freshly prepared solutions of the four different HBDS were small. After the DES absorbed CO₂ without forming carbamate, CO₂ still remained in a molecular state, interacting weakly with the DES. Compared to the fresh solution, the number of hydrogen bonds in the system remained almost unchanged, while the hydrogen bond

lifetime was extended, indicating that the hydrogen bonds-maintained interactions within the system for a longer period.

As the reaction continued and the system reached saturation (1.65 mol CO₂/kg DES), as shown in Figure 11(D), the number of hydrogen bonds in the system peaked at 2869, and the hydrogen bond lifetime increased to 5.84 ps. This suggests that, as the reaction progressed, the newly formed MEACOO⁻ products redistributed the hydrogen bonding network with other species in the system (including MEACOO⁻ and MEAH⁺), and the more abundant the absorption products, the stronger the hydrogen bonding and the more stable the system became.

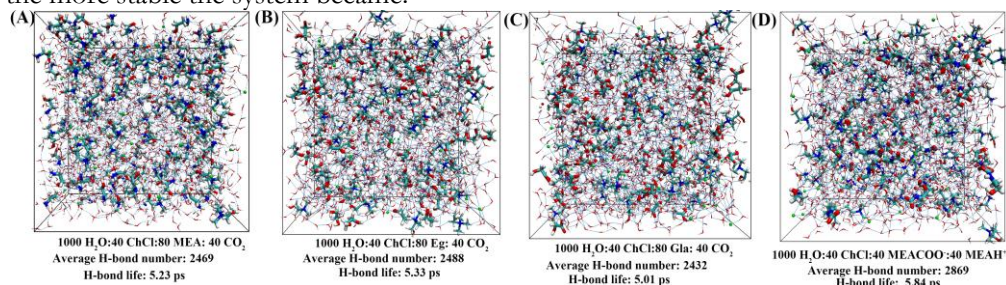


Figure 11: Average number and lifetime of hydrogen bonds in fresh solutions: (A) 30 wt% ChCl-2MEA, (B) 30 wt% ChCl-2Eg, (C) 30 wt% ChCl-2Gla, (D) 30 wt% ChCl-2MEA (1.65 mol CO₂/kg DES).

5. Discussion

This study synthesized a series of DESs containing different HBDs and revealed the reasons behind their differences in CO₂ absorption capacity at the molecular level. Specifically, the CO₂ capture capacity of ChCl-2MEA was significantly higher than that of ChCl-2Gla and ChCl-2Eg. Additionally, the physicochemical properties of DESs before and after CO₂ absorption, as well as their absorption mechanisms, were explored using ¹H NMR, ¹³C NMR, TGA, and DSC. The results indicated that the DESs exhibit high thermal stability. DFT calculations and MD simulations were employed to investigate the internal mechanisms responsible for the significant differences in CO₂ absorption between DESs formed with different HBDs. The results showed that the amine-based HBDs primarily undergo chemical absorption with CO₂, while non-amine HBDs primarily involve weak interactions. Furthermore, the CO₂ absorption capacity was found to be positively correlated with the weak interactions on the DES surface.

Acknowledgment: The authors are grateful for funding from the National Natural Science Foundation of China (51974344) and the National Natural Science Foundation of China (52130401).

References

- Cui, G., Lv, M., & Yang, D. (2019). Efficient CO₂ absorption by azolide-based deep eutectic solvents. *Chemical Communications*, 55(10), 1426-1429.
- Du, J., Yang, W., Xu, L., Chen, J., Song, Z., Wang, B., & Sun, L. (2025). The promotion mechanism of ammonia-based CO₂ capture by hydroxyl and amine additives: A molecular dynamics and DFT study. *Fuel*, 387, 134425.

- Gaussian 16, Revision A.03, Frisch, M., Gaussian 16, Revision A.03, Frisch, M. J., et al., Gaussian, Inc., Wallingford CT, 2016.
- Gu, Y., Hou, Y., Ren, S., Sun, Y., & Wu, W. (2020). Hydrophobic Functional Deep Eutectic Solvents Used for Efficient and Reversible Capture of CO₂. *ACS Omega*, 5(12), 6809-6816.
- Han, S.-C., Sung, H., Noh, H.-W., Mazari, S. A., Moon, J.-H., & Kim, K.-M. (2024). Synergistic effect of blended amines on carbon dioxide absorption: Thermodynamic modeling and analysis of regeneration energy. *Renewable and Sustainable Energy Reviews*, 197, 114362.
- Jafari, H., Noaparast, M., Moghaddam, J., Mohseni, M., & Balesini, A. A. (2025). Effect of water on the deep-eutectic solvent based on the choline chloride and p-toluenesulfonic acid: MD, DFT and experimental studies. *Journal of Molecular Liquids*, 422, 126932.
- Lu, T., & Chen, F. (2012). Multiwfn: A multifunctional wavefunction analyzer. *Journal of Computational Chemistry*, 33(5), 580-592.
- Lukasheva, N. V., Vorobiov, V. K., Andreeva, V. S., Simonova, M. A., Dobrodumov, A. V., & Smirnov, M. A. (2024). Relation of acrylic acid polymerization behavior in deep eutectic solvent to water content: Computer simulation and experiment. *Journal of Molecular Liquids*, 414, 126172.
- Mao, J., Ma, Y., Ci, Y., Liu, J., Li, C., Yang, W., . . . Yun, Y. (2025). Anhydrous deep eutectic solvents-based biphasic absorbents for efficient CO₂ capture: Unravelling the critical role of hydrogen bond-mediated electron transfer. *Chemical Engineering Journal*, 511, 161988.
- Palomar, J., Lemus, J., Navarro, P., Moya, C., Santiago, R., Hospital-Benito, D., & Hernández, E. (2024). Process Simulation and Optimization on Ionic Liquids. *Chemical Reviews*, 124(4), 1649-1737.
- Trivedi, T. J., Lee, J. H., Lee, H. J., Jeong, Y. K., & Choi, J. W. (2016). Deep eutectic solvents as attractive media for CO₂ capture. *Green Chemistry*, 18(9), 2834-2842.
- Valencia-Marquez, D., Flores-Tlacuahuac, A., & Vasquez-Medrano, R. (2017). An optimization approach for CO₂ capture using ionic liquids. *Journal of Cleaner Production*, 168, 1652-1667.
- Wang, C., Zhu, J., Xiao, G., Zhou, X., Wang, H., Zhu, Q., Cao, Y. (2024). Effect of water on CO₂ capture and phase change in non-aqueous 1,4-butanediamine/ethylene glycol biphasic absorbents: Role of hydrogen bond competition. *Chemical Engineering Journal*, 496, 154231.
- Wang, Y., Zhang, W., Ren, S., Hou, Y., & Wu, W. (2024). Rapid Absorption and Desorption of CO₂ by Deep Eutectic Solvents via Reversible CO₂-Triggered Proton Transfer Process. *ACS Sustainable Chemistry & Engineering*, 12(10), 3987-3995.
- Xin, T., Yang, W., Li, S., Xu, C., & Yang, Y. (2025). Development of a novel coal-fueled nearly zero emission semi-closed supercritical CO₂ cycle with the net efficiency above 50 % based on the process splitting method. *Energy*, 318, 134944.
- Zhao, P., Li, Z., Dong, B., Zhang, L., Su, X., Wang, Q., Gao, J. (2025). An enhancement and mechanism of CO₂ capture by a dual-amino porous ionic liquid. *Separation and Purification Technology*, 360, 131064.
- Zhou, S., Zhu, Y., Xi, H., Hao, Z., Han, Z., & Sun, C. (2024). Research on CO₂ capture performance and reaction mechanism using newly tetraethylenepentamine (TEPA)+monoethanolamine (MEA) mixed absorbent for onboard application. *Chemical Engineering Journal*, 485, 149790.